Al-Rafidain Journal of Engineering Sciences

Journal homepage https://rjes.iq/index.php/rjes

ISSN 3005-3153 (Online)

Literature Review on the Use of Basalt Fiber Sheets for Improving Shear Resistance in High-Strength Concrete Beams

Muhaned Dawood Kashash[1] and Nibras Nizar Khalid[2]

[1,2] Department of Civil Engineering, College of Engineering, Al-Mustansiriyah University, 10064 Baghdad, Iraq

ARTICLE INFO

Article history:
Received 25 November 2024
Revised 26 November 2024,
Accepted 22 December 2024,
Available online 23 December 2024

Keywords:
Shear behavior
External Strengthening
High-Strength Concrete (HSC)
Basalt Fiber-Reinforced Polymer (BFRP)
Structural Reinforcement

ABSTRACT

This paper reviewed the application of basalt fiber-reinforced polymer sheets in enhancing the shear strength of reinforced concrete beams .However , traditional reinforcement methods are generally very limited regarding strength, durability, and environmental resistance. This has created a demand for advanced materials such as fiber-reinforced polymers. Basalt fibers have several advantages over conventional carbon and glass fibers owing to their superior mechanical properties, lower environmental impact, and cost-effectiveness. This review made an analysis of the experimental data on the effectiveness of BFRP sheets in enhancing shear capacity in RC beams, with a view to considering parameters such as shear span-to-depth ratios, material modulus of elasticity, and bonding configurations. The result showed that BFRP sheets remarkably enhanced shear resistance and structural ductility, particularly in configurations optimized to prevent premature failure. It also emphasized how further research was lacking, particularly in the performance of HSC reinforced with BFRP under different loading conditions. Results have shown that future studies must be conducted to develop the bonding and reinforcement techniques that can fully realize the benefits of BFRP in advanced structural applications . This work provides an insight into the structural potential of BFRP as a sustainable reinforcement material in modern concrete infrastructure.

1. Introduction

The modern construction sector emphasizes strengthening structures to comply with evolving design standards and increased durability requirements in response to environmental degradation. Structures in challenging settings such as high-traffic areas and corrosive environments exposed to explosive or impact forces—are reinforced to maintain longevity and structural integrity. Conventional reinforcement methods for reinforced concrete (RC) structures include metal plate layering, textile fiber sheets, wire mesh installation, post-tensioning, concrete or steel jacketing, and epoxy injection [1]–[4].

Recent advancements in materials science and engineering have led to the development of innovative retrofitting techniques. One significant advancement is the application of externally bonded (EB) fiber-reinforced polymer (FRP) composites, which have proven highly effective for structural strengthening and rehabilitation [5]. This approach typically employs unidirectional FRP wrapping sheets composed of carbon, glass, or aramid fibers, enhancing confinement reinforcement in reinforced concrete (RC) structures [6]. In recent years, basalt fibers have emerged as a promising alternative due to their favorable physicochemical and mechanical properties, as well as their environmentally sustainable and cost-effective production processes [7].

Corresponding author E-mail address: mdk@uomustansiriyah.edu.iq
https://doi.org/10.61268/aar48246

Basalt fiber production is simpler and more economical than carbon fiber, producing minimal emissions and waste. Basalt, a naturally occurring material, requires few additives; raw basalt is simply washed and melted. As basalt constitutes over 90% of Earth's magmatic rocks, raw material costs are minimal, comprising only 5–7% of total production expenses. As a result, basalt fabrics cost approximately 20% of carbon fiber fabrics [8],[9].

While basalt fibers are slightly more expensive than glass fibers, they offer a compelling alternative due to their economical production (lower energy and additive requirements) and superior mechanical properties. Basalt fibers provide high strength, ductility, and notable resistance to harsh environments (alkaline, acidic, and saline), making them suitable for applications in concrete reinforcement, bridges, and coastal infrastructure [8], [10], [11].

Experimental studies indicate that basalt fiber/epoxy composites possess a 40% higher strength-to-weight ratio and 20% greater specific stiffness compared to E-glass/epoxy composites under similar conditions. Basalt composites also demonstrate excellent interlaminar shear strength, indicating strong fiber-matrix adhesion, along with thermal insulation and fire resistance. Unlike carbon fibers, basalt fibers are electrically non-conductive, preventing galvanic corrosion when combined with metals [8]. This combination of cost-efficiency and outstanding performance makes basalt fiber composites a significant advancement for concrete structure rehabilitation.

2. Background on Fiber Reinforced Polymers (FRPs)

Fiber reinforcements are crucial in enhancing structural durability due to their light weight, corrosion resistance, and directional stiffness, making them ideal for structural reinforcement. This section highlights the characteristics and distinctions among four primary fibers used in concrete reinforcement: carbon, glass, aramid, and basalt.

2.1 Fiber Types

*1. Carbon Fibers***:** Carbon fibers are renowned for their high tensile strength (3,500 to 6,000 MPa) and elastic modulus (230 to 600 GPa), which result from their aligned structure and high crystallization. However, their low elongation at failure (0.5–1.1%) and high production costs—owing to complex processes like oxidation, carbonization, and graphitization—limit their application [12], [13].

2. Glass Fibers: Widely used in composites, glass fibers are cost-effective, electrically insulating, and easy to apply near electrical infrastructure. E-glass, the most common type, is affordable and offers good insulation, while S-glass, with higher tensile strength and modulus, is suited for aerospace at a higher cost. However, non-alkali-resistant types degrade in alkaline and moist environments [12], [14].

3. Aramid Fibers: First produced in 1971, aramid fibers (e.g., Kevlar by DuPont, Technora by Teijin, Twaron by Akzo Nobel) are highly durable and retain over 80% of their strength up to 180°C. Kevlar comes in specialized grades, such as Kevlar 29 for impact resistance and Kevlar 49 for composites. Unique for their nonlinear, ductile compression behavior, aramids offer enhanced toughness but are sensitive to UV light, absorb moisture, and degrade with certain chemicals [15], [16].

4. Basalt Fibers: Basalt fibers, derived from volcanic rock, are an eco-friendly, cost-effective alternative to glass fibers, offering excellent thermal stability (up to 750°C), chemical resistance, and low moisture absorption. While their production requires more energy, basalt's abundant raw materials help control costs. Basalt fibers match or exceed E-glass properties and sometimes approach those of the more expensive S-glass, making them a sustainable choice for applications where performance and environmental considerations are priorities [12], [13] .

2.2 Advantages and Disadvantages of FRP Materials

FRP materials are widely used in engineering for their unique properties, but their advantages and limitations require careful consideration in design and application[17].

Advantages:

- ✓ Easier handling and installation compared to steel
- ✓ Excellent resistance with corrosion
- ✓ Requires little maintenance
- ✓ Exceptional durability and flexibility
- ✓ High ultimate strength compared to steel (2-3 times greater)
- ✓ Low density contributing to a superior strength-to-weight ratio

Disadvantages:

- ☒ High cost
- ☒ Low modulus of elasticity
- ☒ Risk of fire or accidental damage (unless properly protected)
- ☒ Relatively low transverse strength
- ☒ Long-term durability is not yet fully established

2.3 Manufacturing Process

Basalt fiber production uses a continuous filament spinning process similar to how glass fibers are manufactured. This provides a cost advantage by leveraging existing glass fiber infrastructure. The process involves several key steps: raw material preparation where basalt rocks are crushed, screened, washed and dried. The basalt was subsequently melted at approximately 1450°C in an electrical furnace. The melt flows into a temperature controlled forehearth and then is distributed to the spinnerets. As shown in Figure. 1 , as the melt is extruded through fine nozzles, continuous filaments are formed which are sized and wound onto rolls[13].

The basalt fibers can then be converted into various products as depicted in Figure. 2 The continuous strands may be twisted into yarns, cut for use in composites or woven into fabrics. This flexibility expands the applications of basalt fibers [13] .

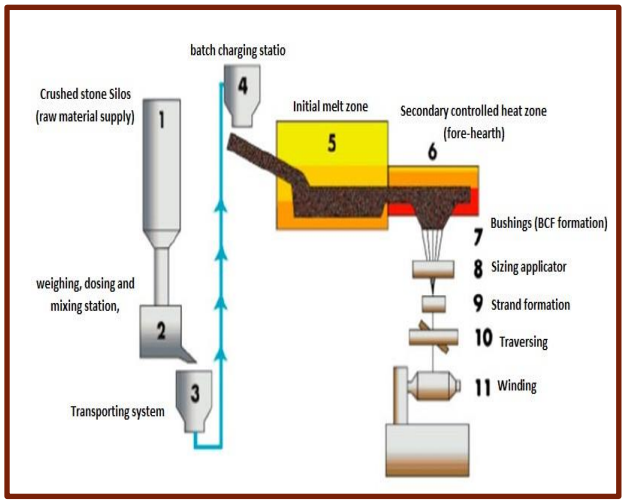

Figure 1. A Simplified Scheme of a Basalt Fibreization Processing Line [13]**.**

Figure 2. Some basalt fiber product [13]

3. High strength concrete

HSC is defined as having a specified compressive strength of 8000 psi (55 MPa) or greater , according to **ACI 363.2R-11**[18] . While production methods are similar to regular concrete, stricter quality control and testing are necessary for HSC. The growing demand for durable, high-performance structures has driven the increased use of HSC. However, effectively producing and utilizing HSC requires understanding its unique properties, production requirements, and structural behavior, especially the flexural and shear performance of HSC beams under loading conditions. Optimizing the design and ensuring structural integrity of HSC members relies on this knowledge

3.1 Production of High Strength Concrete

Many experimental studies on mix design for HSC with silica fume to determine the best mix proportion for used materials of which:

Al-Mashhadi and Hekmat (2014) [19] developed mix proportioning method for HSC with compressive strengths of 41-90 MPa incorporating 5-15% silica fume as cement replacement. The total cementitious materials content is fixed at 520 kg/m3 along with superplasticizer dosage to achieve a target slump of 50-75mm. Selection tables are provided to choose parameters including maximum aggregate size, water-cementitious ratio, percentage silica fume and air content based on desired strength. The approach allows flexibility in materials selection as per local availability. Several trial batches were analyzed to validate and refine the initial proposed guidelines. Test results demonstrated enhanced workability, reduced bleeding and segregation, besides substantially higher compressive strength compared to conventional HSC mixes. The simple design procedure can help produce reliable, cost-effective high performance HSC incorporating silica fume to better utilize industrial by-products.

In 2006, Yaqub and Bukhari[20] presented an experimental study that included the development of a concrete mix design. The advancement of mix design techniques plays a key role in concrete innovation, as it involves determining experimentally the optimal concrete mixes to maximize strength while minimizing costs. In their study, locally available concrete ingredients were selected to ascertain the relative proportions needed for optimal results. Four mixes were chosen with the goal of achieving compressive strength over 162 MPa. The variables were mix ratio and aggregate size. Four mixing ratios by weight were selected, all with a 0.3 w/c ratio. Ultra 727 superplasticizers were utilized to improve workability. The results indicate that compressive strength depends on mix proportion, aggregate texture and size, and compaction method. Furthermore, it was found that a 1:0.75:1.5 ratio exhibited greater strength compared to the other three mix proportions tested.

Annadurai and Ravichandran (2014) [21] conducted a comprehensive study on developing high strength concrete mixtures utilizing high range water reducing admixtures and silica fume. Their experimental methodology aimed to determine the optimal combination of locally sourced ingredients, including river sand, 53 grade Portland cement, and 10mm maximum size coarse aggregates per ASTM C127 standards, to achieve a target compressive strength of 60MPa. Guided by ACI 211.4R-93, five mix designs were tested - one control mix with 0.5% (High Range Water Reducers) HRWR sans silica fume, and four mixes with silica fume quantities ranging from 6-9% of cementitious materials by weight. The HRWR dosage also varied across these four mixes, increasing incrementally by 0.1% from 0.6-0.9%. Specimens were cured for 28 days prior to compressive strength testing.

Key findings were:

- The fineness modulus of the fine aggregate, set at 3.0 for all mixes per preliminary testing, is critical for high strength concrete development.
- Increasing the silica fume replacement level from 0-9% yielded significant compressive strength gains, however this also reduced workability/slump.

9% silica fume replacement paired with 0.9% HRWR produced the maximum compressive strength.

3.2 Flexural and Shear Behavior of HSC Beams

Cladera and Marí (2005) [22] tested 18 reinforced HSC beams with compressive strengths from 50-87 MPa to study the influence of parameters like the concrete strength, amount of transverse and longitudinal reinforcement, and distributed longitudinal reinforcement on shear behavior and strength. Beams without stirrups showed sudden, brittle shear failures. Adding stirrups resulted in a more ductile response and changed the cracking patterns and failure mode. In general, shear strength increased with increasing concrete strength for beams with stirrups, indicating they were more effective at higher strengths. The minimum proposed stirrup amount was sufficient to provide adequate strength reserve after cracking.

The authors also compared the test results to various code equations, finding better correlation with models based on modified compression field theory.

Campione et al. (2014) [23] investigated the flexural and shear behavior of HSC beams with longitudinal reinforcement and stirrups. The study found that while the flexural strength is not significantly increased in HSC beams compared to normal-strength concrete (NSC) beams , the shear strength is enhanced due to the higher concrete compressive strength. However, HSC exhibits a more brittle shear failure through aggregates as the paste strength increases, reducing aggregate interlock . With higher reinforcement ratios and reduced stirrup spacing, shear failures become more ductile and transition to flexural failure. The shear span-to-depth ratio also affects the failure mode. Analytical models were developed to predict flexural and shear capacities based on parameters like concrete strength, reinforcement ratio and shear span. The models showed good agreement with experimental results.

In comparison, **Campione and Mindess (1999)** [24] and **Campione et al. (2003)** [25] conducted experimental studies on HSC beams.As shown in Figure 2.1, the load deflection curves of beams tested at different a/d ratios of 2.25, 2.0, and 2.8. At higher stirrup spacings, brittle shear failure was observed, as indicated by sudden load drops. At lower stirrup spacings, a transition from brittle diagonal tension shear failure to ductile flexural failure was observed. The curves demonstrate the role of stirrups in bridging the shear cracks.

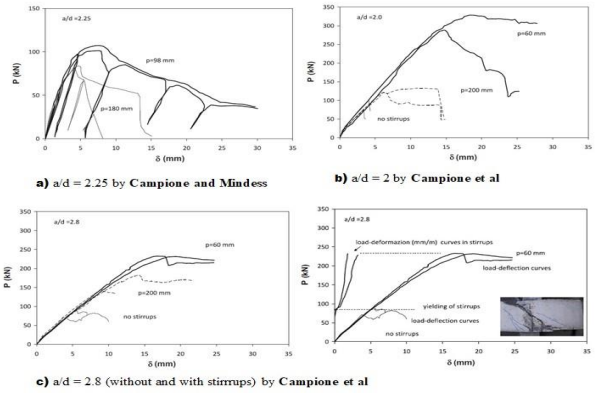

Figure 3. Load-deflection curves of tested beams [23]

Kim et al. (2017)[26] conducted a comprehensive study to develop an improved shear strength prediction approach for reinforced concrete beams without shear reinforcement. Their innovative model considered the impact of the bond action between the longitudinal reinforcement and concrete, a vital factor that was overlooked in earlier models. The experimental program consisted of testing concrete beams with varying shear span-to-depth ratios ranging from 2.0 to 4.0, different concrete compressive strengths, tension reinforcement ratios, and effective depths. The researchers suggested an equation to predict the distance from the support to the location of the final flexural crack, which matched closely with experimental findings. Their analytical model quantified the shear contributions from the concrete compressive zone, the dowel action considering the bond behavior of the longitudinal reinforcement, and the aggregate interlock mechanism. The model estimated the shear contribution of the concrete compressive zone to be (47-57%) of the total shear force, the shear force due to dowel action considering bond action to be (25-30%), and the shear force due to aggregate interlock to be (18-30 %). The proposed method for predicting shear strength , which explicitly included the bond action of the longitudinal reinforcement ,showed superior accuracy compared to existing models, providing reasonable predictions for previous experimental results with an average ratio of 0.96 and a coefficient of variation of (14.5%).

4. Shear Behavior of Beams without Stirrups

The shear failure mechanism in reinforced concrete beams without shear reinforcement is an important topic in structural engineering. In these beams, shear resistance is assumed to be transmitted through the web zone of the concrete. The concrete contributes a part of the shear resistance, while the shear reinforcement is expected to provide the remaining part in beams with shear reinforcement. Shear stresses are defined as stresses parallel or tangential to the beam section. When a simply supported beam bends, the fibers above the neutral axis are

compressed, while those below the neutral axis are tensioned. When reinforced concrete beams with longitudinal reinforcement are subjected to external loads, diagonal tensile stresses develop, which can lead to cracks. These cracks are vertical in the middle of the beam and become inclined as they approach the beapm support. Diagonal tension stresses are responsible for causing the inclined cracks in the beams. If the member's resistance to diagonal tension is less than its resistance to flexural tension, diagonal tension cracks may cause the beam to fail. This kind of crack typically starts with a few vertical flexural cracks in the middle of the beam, followed by the separation of the bond between the longitudinal reinforcement and the surrounding concrete at the support. Eventually, two or three inclined cracks appear at a distance of 1/2 to 2d from the support face **(Slowik, 2014)** [27] .

When concrete beams are subjected to bending moments exceeding the modulus of rupture of concrete $\left(f_r = 7.5\lambda\sqrt{f'_c}\right)$, vertical flexural cracks initiate at the location of maximum bending stress. As the load increases, inclined cracks subsequently develop in the web region, in close proximity to the supports. The shear resistance in reinforced concrete beams without shear reinforcement is attributed to a combination of mechanisms, as described by **M. N. Hassoun and A. Al-Manaseer (2020)** [28]:

1. Shear resistance of uncracked concrete (V_z): The uncracked portion of the concrete contributes to the shear resistance through its inherent tensile strength.
2. Interface shear transfer (V_a): The rough surfaces along the crack interface interlock, providing resistance to shear forces through aggregate interlock tangentially.
3. Arch action: An internal arching mechanism within the beam can contribute to shear resistance, particularly in deep beams.
4. Dowel action (V_d): The longitudinal reinforcing bars act as dowels, resisting the transverse shearing forces and providing additional shear resistance.

In the absence of shear reinforcement in rectangular beams, the proportions of shear resistance contributed by these mechanisms are typically 20 to 40% by V_z, 35 to 50% by V_a, and 15 to 25% by V_d . As shown in Figure. 3 below, the shear failure mechanisms and the forces involved are illustrated, including the general form (a), web-shear crack (b), flexural-shear crack (c), and the analysis of forces V_a, V_z, and V_d (d).

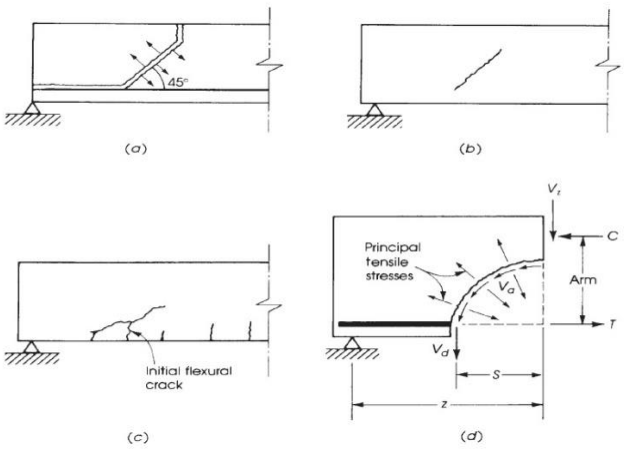

Figure 4. Shear failure: (a) general form, (b) web-shear crack, (c) flexural-shear crack, (d) analysis of forces involved in shear ($\mathbf{V_a}$ = interface shear, $\mathbf{V_z}$= shear resistance, $\mathbf{V_d}$ = dowel force) [28]

Schmidt et al. (2021) [29] described the mechanism of shear failure in beams without shear reinforcement as a complex interplay of various shear transfer actions. According to their Shear Crack Propagation Theory (SCPT), the shear resistance of such members is provided by the combined contribution of several mechanisms, including the uncracked concrete zone (contributing up to 100% at low load levels and reducing to around 30% near failure), fracture process zone, aggregate interlock (becoming the most effective shear-carrying mechanism at around 40% near failure), dowel action, and crack bridging actions. The relative significance of each mechanism varies throughout the loading process, with the uncracked concrete zone being the most dominant at low load levels, while aggregate interlock becomes the most effective shear-carrying mechanism at higher loads approaching failure. The theory accommodates the equilibrium of forces, material constitutive behavior, and

kinematic compatibility that permits a detailed analysis of the ever-changing interplay in the propagation of the crack, stress evolution, and activation of all the various transferred shear actions in the developing shear crack.

Bernat et al. (2020) [30]. A mechanical model was developed for predicting the shear strength of SFRC beams without stirrups. The model expands on the Multi-Action Shear Model, which considers several contributions of shear-resisting mechanisms: (a) the uncracked compressed concrete chord, (b) the diagonally cracked web, and (c) the stirrups crossing the critical shear crack, in the case these are provided, as well as (d) the longitudinal reinforcement. **Cavagnis et al. (2015)** [31]. They further noted that the aggregate interlock significantly contributes to the shear resistance in reinforced concrete beams without shear reinforcement because of the crack geometry and kinematics. Using detailed photogrammetric measurements, it was observed that the failure plane in tension was capable of rereleasing interface shear stresses, and as a consequence, the vertical upper parts of the critical shear cracks may carry more shear forces because of the activation. The crack opening and sliding are the significant factors that were said to be relied upon for the aggregate interlock. They also noted that with an increase in the crack size and the sliding, a decrease in the aggregate interlock stresses occurred. Also , they stated that the new cracking mechanism developed from the existing critical shear crack, causing aggregate interlock capacity loss and failure. The study pointed out that for a proper assessment of the role of aggregate interlock in shear strength , careful consideration must be given to the actual cracking pattern and its kinematics during the failure process, as well as other potential shear-transfer actions.

Arowojolu et al. (2021) [32] The objective was to examine the impact of the shear span-to-effective depth ratio (a/d) on the performance of HSC beams. The research included the testing of six HSC beam samples, both with and without shear reinforcement , subjected to four-point bending. The a/d ratio was adjusted between (2.0) and (3.0) . The researchers examined the cracking moments, moment capacities, load-deflection behavior, and shear strengths of the beams. The results showed that the a/d ratio had a higher influence on the shear strength of beams without shear reinforcement compared to those with shear reinforcement. Most of the existing shear resistance prediction models underestimated the concrete shear strength for beams without shear reinforcement but overestimated the shear resistance for beams with shear reinforcement. However, the fib Model Code 2010 accurately predicted the shear resistance for all the beams within an appropriate level of approximation. The authors concluded that the a/d ratio, in addition to aggregate interlock, should be accounted for in shear prediction models , especially for HSC construction.

Þórhallsson and Birgisson (2014) [33] conducted an experimental study to compare the shear strength of concrete beams without shear reinforcement with various building codes, including the American Concrete Institution (ACI) Building Code, European Standard Eurocode 2 (EC2), and Model Code 2010. The researchers tested eighteen reinforced concrete beams without shear reinforcement, varying the beam height (105, 131, 164, 189, 236, and 335 mm) and the longitudinal reinforcement ratio (1.31% to 1.55%). The main variable investigated was the shear span-to-effective depth ratio (a/d). The researchers measured the shear force at the first shear crack and the ultimate shear force at failure. The results showed that the three building codes provided different estimates for shear resistance. The EC2 and Model Code 2010 calculated the shear design value lower than the value when the first shear crack appeared, while the ACI code gave the lowest estimate of shear resistance, being on the conservative side. The new shear approximations in Model Code 2010 yielded 5% to 20% lower values than those calculated according to EC2. The authors concluded that, although all codes were safe for design purposes, the ACI code was the most conservative, and the improvements made to the EC2 shear resistance equation resulted in better estimates of the actual shear resistance, especially for deeper beams.

S.V.T. Janaka Perera and Hiroshi Mutsuyoshi (2013) [34] A detailed study was

conducted on the shear behavior of beams without stirrups, in particular, an estimate of the diagonal cracking shear strength of reinforced HSC members without any form of web reinforcement. The main objective of their study was to propose a simple and precise equation to predict the diagonal cracking shear strength of beams by considering the effects of both aggregate and concrete strengths. Many vital parameters have been investigated by the authors, such as shear span-to-depth ratio (a/d) from 2.5 to 9.05, primary longitudinal reinforcement ratio (ρ) from 0.47% to 3.39%, adequate depth (d) from 132 mm to 1097 mm, and concrete compressive strength (f'c) from 10.5 MPa to 193.8 MPa, through parametric study and meticulous comparison against large arrays of experimental data obtained from previous investigations

The key findings and conclusions were:

- That HSC strength is primarily controlled by the diagonal crack shear strength obtained by the ratio between uniaxial compressive strength to tensile strength, Ductility Number (DN)of concrete, relative to that of aggregate.
- Three concrete strength regions were proposed, which include: Normal Strength Concrete (NSC, f'c ≤ 60 MPa), Optimal Strength Concrete (OSC, 60 MPa < f'c < 100 MPa), and High Strength Concrete (HSC, f'c ≥ 100 MPa).
- A shear strength prediction equation (Eq. 1) was developed, considering a/d, ρ, f'c, and d. This proposed formula estimated the diagonal cracking shear strength of slender RC beams without web reinforcement quite accurately for the wide range of concrete strengths between 10.5 and 193.8 MPa.

$$v_{cr} = f_v\,(1000\rho)^{1/3}\,d^{-1/4}\left(a/d - 1\right)^{-1/6} \quad \text{... (1)}$$

where,

$$f_v = 0.49\,f'c^{\frac{1}{6}}, for\ \ f'c \le 60\ MPa$$

$$f_v = 0.97\ \ , for\ 60\ MPa < f'c < 100\ MPa$$

$$f_v = 2.06\,f'c^{\frac{-1}{6}}, f'c \ge 100\ MPa$$

- The authors concluded that "the current code provisions (JSCE and ACI), as well as the proposed ones for evaluating the shear strength of HSC beams without web reinforcement, need to be modified.

In their study on the shear behavior of (MRPLWC) beams without the presence of shear reinforcement, **AlSaraj et al. (2019)** [35] shed some light on the mechanism of shear failure in such beams. Tests were conducted by researchers on nine (MRPLWC) beams through a two-point loading test, factoring in variables such as volume fraction of steel fibers (Vf), the ratio of longitudinal reinforcement (ρ), and shear span to effective depth (a/d). The researchers found that the a/d ratio and Vf influenced the mode of failure. Beams with (a/d) of 2.5 have failed in shear, and a/d ratios of 3.5 and 4.0 all have been unable in diagonal tension except those with higher Vf (2.0%) with a/d of 4.0 which showed failure by shear-flexure. The authors observed that increasing the a/d ratio and Vf resulted in a change in the failure mode from diagonal tension failure to shear-flexural failure. Furthermore, they noted that the ultimate loads were significantly higher than the inclined cracking loads, ranging from 190.9% to 272%, for beams with a/d ratios between 2.5 and 4.0, longitudinal reinforcement ratios varying from 3.29% to 5.23%, and Vf varying from 0.0% to 2.0%.

5. Basalt fiber reinforced polymer (BFRP)

Basalt fiber sheets are a type of natural fiber reinforcement that has emerged as an alternative to traditional glass and carbon fibers for polymer matrix composites. Basalt fibers are produced from volcanic rock through a process similar to glass fiber manufacturing **(Plappert et al., 2020)** [36]. Compared to glass fibers, basalt fibers have higher strength and stiffness properties with tensile strength ranging from (2000-4800 Mpa), elastic modulus of (89-110 Gpa) and elongation at break of 3-3.2% **(Yuan et al., 2018)**[37]. Additionally , basalt fibers have better chemical and thermal stability than glass fibers . The production of basalt fibers requires less energy and has lower emissions than carbon and glass fibers making it an environmentally friendly option **(Yuan et al., 2018)** [37] .

Several studies have investigated the

mechanical properties of basalt fiber -reinforced polymer composites. **Yuan et al. (2018)**[37] examined the bond behavior between basalt fiber sheets and steel fiber reinforced concrete (SFRC). The basalt fiber sheets were made of unidirectional fibers with (300 g/m2) areal weight embedded in an epoxy resin matrix. Single-lap shear tests were conducted on concrete specimens with varying steel fiber volume fractions from 0-1.0%. The results showed 31-76% increase in peak interfacial shear stress for SFRC compared to plain concrete. The debonding process was more ductile with SFRC due to the pull-out resistance of steel fibers. The interfacial fracture toughness also increased proportionally with higher steel fiber volume. The authors proposed analytical models to predict the bond strength and interfacial shear stress incorporating the steel fiber volume fraction.

Plappert et al. (2020) [36] conducted a comprehensive characterization of the mechanical properties of autoclavecured unidirectional basalt fiber/epoxy composites. Tensile, compressive and shear properties were measured based on standardized testing methods. The results showed a tensile strength of (1310 MPa), compressive strength of (776 MPa) and shear strength of (50.5 MPa). The properties were comparable or slightly higher than E-glass composites. However, the shear strength was lower than glass composites, indicating weak fiber-matrix adhesion. Scanning electron microscopy of fractured surfaces revealed smooth debonded areas on the fibers, confirming poor interface bonding. Surface modification of fibers was recommended to improve the adhesion.

Focusing on the potential of basalt fiber reinforcement for improved shear capacity and crack control in concrete beams, this collection of studies delves into the critical mechanical properties and thermal resistance that underpin this material's effectiveness. **Jianbing et al. (2022)** [38] evaluated the shear performance of basalt fiber concrete beams without web reinforcement through four-point bending tests. Partial replacement of regular concrete with basalt fiber concrete was examined. The results showed 25-40% increase in cracking load with addition of basalt fibers. The concrete beam fully reinforced with basalt fiber concrete experienced bending failure with 15% higher ultimate load capacity compared to regular concrete. Finite element modeling was conducted to simulate the failure modes and load-deflection response. The study demonstrated that proper integration of basalt fibers in concrete beams can enhance the shear performance.

He et al. (2020) [39] tested RC beams strengthened in shear with BFRP grids attached using polymer cement mortar. Results showed that the strengthening was effective in increasing the shear capacity, with 40.9-47.1% gains for shear span ratios from 1.6 to 2.4. The study also found "the contribution of the BFRP grids to the shear capacity was not sensitive to the shear span ratio." Angled 45° grid orientation provided improved crack control compared to 0° alignment.

Osman (2023) [40] used finite element models to evaluate the influences of parameters like beam depth, concrete strength, and FRP thickness on shear strengthening per different guidelines. Models showed reasonable correlation with experimental results. The author concluded that "the ACI guideline showed acceptable differences compared with the other guidelines" in predicting shear capacity of FRP-strengthened RC beams.

6. Flexural strengthening of Reinforced Concrete (RC) Beams with BFRP

Chaudhari and Gorade (2023)[41] experimentally investigated the use of externally bonded BFRP fabrics to strengthen RC beams in flexure. A total of 9 RC beams were tested under 4-point bending, including 1 control beam without strengthening and 8 beams wrapped with BFRP in different configurations like full wrapping, inclined strip wrapping, vertical strip wrapping, and bottom strip wrapping. The results showed that full wrapping with BFRP provided the maximum gains, increasing the flexural strength by (59.5%) and load carrying capacity by (60%) compared to the control beam. The inclined and vertical strip wrapped beams also exhibited improved strength and capacity over the control. The study

demonstrated that externally bonding BFRP fabrics can significantly enhance the flexural performance of RC beams, with full wrapping being the most effective configuration.

Hughes et al. (2020)[42] conducted an experimental study on the flexural strengthening of RC beams using BFRP fabrics. They tested five full-scale RC beams under 4-point bending, with different numbers of BFRP layers (0, 2, 4, 6 and 8). They found that BFRP fabrics significantly improved the yield and ultimate load capacity of the RC beams, up to (37%) and (92%) respectively. They also observed that the displacement at ultimate load increased with BFRP layers, up to (54%), while the displacement at yield remained almost constant. The failure mode of the beams changed from ductile flexure to brittle shear when 8 BFRP layers were used, indicating over-strengthening. They concluded that BFRP fabrics are a promising technique for flexural strengthening of RC beams, as long as the number of BFRP layers is optimized to avoid sudden shear failure.

Chen et al. (2018) [43]evaluated the flexural strengthening of RC beams using BFRP fabrics with different wrapping schemes , anchorage systems, and epoxy adhesives . They found that BFRP U-jackets improved the load-carrying capacity and ductility of the RC beams by preventing FRP debonding and utilizing the high tensile strength of BFRP. They also observed that 45°inclined U-jackets were more effective than vertical U-jackets, and that the type of epoxy adhesive influenced ductility more than strength. They suggested that BFRP is a cost-effective and environmentally friendly alternative to carbon or glass FRP for flexural strengthening of RC beams ,especially when the very high-strength of carbon FRP is not needed. They recommended further research on the dynamic loading behavior of BFRP-strengthened beams.

Surwase et al. (2019)[44] investigated the flexural behavior of RC T-beams strengthened with BFRP sheets in different configurations. They tested 7 RC T-beams ,including one control beam and 6 beams with BFRP sheets bonded externally. They found that BFRP sheets enhanced the ultimate load capacity and reduced the deflection of the strengthened beams. The most effective strengthening scheme was the U-wrapped BFRP sheet in the middle region, which increased the load capacity by (37.5%) compared to the control beam . The study showed that BFRP sheets are a viable technique for flexural strengthening of RC T-beams .

Kadhim et al. (2019) [45] used finite element modeling to analyze the strengthening and rehabilitation of corroded RC beams using BFRP sheets. Eight full-scale RC beam models were developed with different parameters including corrosion level, BFRP wrapping schemes, and number of BFRP layers. The models were validated by comparison to experimental results from literature, showing good agreement. It was found that BFRP strengthening increased the ultimate load capacity even with 20% corrosion of the steel rebar. Eight BFRP layers with bottom wrapping provided the maximum 14.8% strength increase over an unstrengthened beam. However, BFRP strengthening reduced the ductility of the beams. The study demonstrated using BFRP sheets to strengthen and rehabilitate corroded RC beams was effective in restoring strength, though at the expense of ductility. The finite element approach was able to effectively simulate the structural response of RC beams strengthened with BFRP composites.

7. Shear Strengthening Using FRP

Shear failure in reinforced concrete (RC) beams can occur suddenly and in a brittle manner without warning. Therefore, shear strengthening of existing deficient RC beams is an important issue in structural engineering. Traditionally, shear strengthening has been carried out using steel plates or RC jackets. However, fiber reinforced polymer (FRP) composites have emerged as an effective alternative for shear strengthening due to their high strength-to-weight ratio, corrosion resistance, and ease of application **(Chen et al., 2018)** [43]

7.1 Previous Research on FRP Shear Strengthening

Al-Mussaue and Al-Modhafer (2011)[46] conducted experimental and analytical investigations on the behavior of concrete beams strengthened in shear using CFRP sheets . Twelve reinforced concrete beams were tested under two-point loading with the parameters being concrete strength and CFRP strengthening configuration (shear only or shear and flexure). The beams strengthened with CFRP sheets in both shear and flexure showed higher increases in ultimate load capacity compared to beams strengthened in shear only. The failure mode was dominated by rupture of the CFRP sheets. Finite element analysis was also conducted and showed good agreement with the experimental results. The study demonstrated that externally bonded CFRPsheets can significantly enhance the shear and flexural capacities of RC beams .

Chaallal et al. (1998) [47] tested eight reinforced concrete beams , including two control beams designed for full shear strength, two under-reinforced beams and four beams strengthened in shear using CFRP strips externally bonded on the side faces. The CFRP strips were oriented either vertically or diagonally at 45 degrees. The results showed that the externally bonded CFRP strips increased the shear strength and stiffness of the reinforced concrete beams by reducing shear cracking. The beams with diagonal CFRP strips performed better than those with vertical strips in terms of crack propagation, stiffness and ultimate shear strength. However, the diagonal strips were more susceptible to concrete peel off failure at the strip ends due to stress concentrations. The study demonstrated the feasibility of using externally bonded CFRP side strips for shear strengthening of reinforced concrete beams .

Suparp et al. (2019) [48]conducted a study ,on enhancing the shear capacity of RC beams by incorporating polyester ropes(PR). Five small-scale reinforced concrete beams were tested under four-point bending, including one unstrengthened control beam and four beams strengthened in shear using PR in different configurations and thicknesses. The results showed that applying PR significantly increased the ultimate load carrying capacity compared to the unstrengthened control beam. Increasing the number of PR layers further improved the strengthening effect. The configuration where PR was applied over the full shear span was more effective than strips of PR . The study demonstrated that PR can effectively enhance the shear strength of RC beams when applied externally with epoxy resin .

Mhanna et al. (2019) [49]experimentally investigated and compared the performance of U-wrapped and completely wrapped CFRP strengthening schemes for RC beams deficient in shear. A total of six beams were tested, including two control beams, one beam strengthened with U-wrapped CFRP , two beams strengthened with complete CFRP wrapping, one with depth equal to the U-wrapped beam's web depth and another with depth equal to the U-wrapped beam's total depth. The results showed that while U-wrapping increased shear capacity, complete wrapping provided superior strength enhancement and ductility over U-wrapping for beams of equal depth. The study demonstrated that complete wrapping is the ideal CFRP shear strengthening scheme but U-wrapping can also be effective when complete wrapping is not feasible, however anchors may be required to prevent premature debonding failure.

Panigrahi et al. (2014)[50] experimentally tested 12 RC T-beams, including 1 control beam and 11 beams strengthened in shear using various configurations of externally bonded GFRP sheets. The parameters studied were GFRP amount and distribution, bonded surface, number of layers and fiber orientation. The results showed that externally bonded GFRPsheets can effectively increase the shear capacity of RCT-beams compared to unstrengthened beams. Inclined fibers at 45°performed better than vertical fibers. Anchoring the GFRP sheets using a steel bolt arrangement prevented premature debonding failure and allowed better utilization of the GFRP strength. U- wrapping with end anchors was the most efficient strengthening scheme among those tested . The study demonstrated that external GFRP sheets can enhance the shear

strength of RCT-beams, with the efficiency depending on the fiber orientation, wrap- ping scheme, use of anchorage and other parameters.

AlShadidi et al. (2016)[51] experimentally tested 10 high strength concrete beams under shear loading, including 2 steel reinforced control beams, 2 beams with steel stirrups, and 6 GFRP longitudinally reinforced beams strengthened in shear using various configurations of externally bonded CFRP sheets/strips. The shear strengthening schemes used were full side sheets, U-strips, vertical side strips, and diagonal side strips. Additionally, 0%, 0.5%, and 1% steel fiber content by volume was incorporated in the concrete mix. The results showed that while steel stirrups were still most effective in increasing shear capacity, CFRP U-strips provided comparable strength enhancement of about 85% that of stirrups. A combination of U-strips and 1% steel fiber performed even better than stirrups, allowing a 24% increase in ultimate load over GFRP reinforced beams with stirrups. The study demonstrated that for cases where lack of shear steel is necessitated , external bonding of CFRP U-strips together with sufficient steel fiber content can effectively enhance the shear strength of concrete beams.

7.2 FRP Shear Strength Models

7.2.1 ACI 440.2R Guidelines on FRP Shear Strengthening[52]

The ACI 440.2R standard offers widely accepted design guidance for externally bonded FRP concrete strengthening systems. Applying reliability-based limit states concepts from ACI 318, it defines satisfactory safety margins for avoiding serviceability issues like excessive cracking and ultimate failure modes. FRP contributions are intentionally reduced by calibrated factors to achieve suitable probability of failure metrics.

7.2.1.1 Wrapping schemes

Figure. 5 Illustrates Common FRP Shear Strengthening Layouts Fully encasing members in FRP maximizes strengthening efficiency and is predominantly utilized for columns where all sides are accessible. For beams, slabs can impede full wraps so alternatives exist - 3-sided U-shaped configurations with FRP on the available faces or 2-sided strips bonded on opposite sides. Though successively less efficient, these partial FRP systems still enhance shear capacity compared to an unstrengthened member according to **ACI 440.2R** [52] provisions. Their feasibility provides strengthening options even where construction constraints prevent optimum fiber placement.

7.2.1.2 Nominal shear strength:

The guidelines use existing ACI 318 models for steel reinforcement to estimate the potential shear strengthening of FRP systems. The methodology follows a similar approach as steel, but instead of a fixed yield stress value, an adjustable effective FRP stress term is used. This effective stress takes into account the level of strain that can be achieved in the fibers, as specified in Figure. 5.

Figure 5. Typical wrapping schemes for shear strengthening of concrete beams using FRP laminates

Figure. 6 summarize the equations and variables provided in ACI 440.2R for calculating FRP shear strength. These equations and variables are used to predict the total reinforced shear capacity. By aligning with established methodologies for steel reinforcement, the provisions aim to accurately assess the additional shear resistance provided by FRP materials.

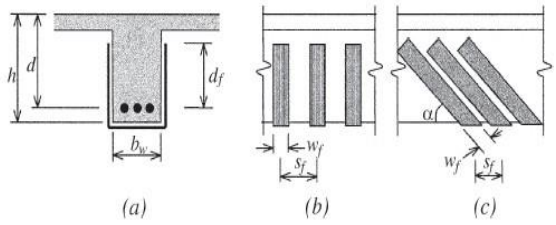

Figure 6. Description of the variables used in shear strengthening calculations for using FRP laminates

7.2.1.3 Shear strength using procedures of ACI 440.2R

$$v_n = \emptyset \left(v_c + v_s + \psi_f v_f\right) \text{.....(2)}$$

where v_c , v_s , v_f = concrete , steel, and FRP shear contributions
$\emptyset$ = strength reduction factor = 0.75
ψ = additional reduction factors for FRP shear reinforcement
0.95: completely wrapped member
0.85: U-wrap and 2 sided schemes

$$v_c = 0.17\,\lambda\sqrt{f'c}\,b_w d \text{.....(3)}$$

$$v_s = \frac{A_{sv} f_{sy} (sin\alpha s + cos\alpha s) d}{s} \text{.....(4)}$$

αs: inclination of stirrups from axis of member

$$v_f = \frac{A_{vf} f_{fe} (sin\alpha + cos\alpha) d_{fv}}{s_f} \text{.....(5)}$$

α: inclination of FRP fiber from axis of member

$$v_f = \frac{A_{vf}\, f_{fe}\, d_{fv}}{s_f} \quad \alpha = 90^\circ \text{ ..... (6)}$$

$$A_{vf} = 2nt_f w_f \text{ ..... (7)}$$

$$f_{fe} = \varepsilon_{fe} E_f \text{ ..... (8)}$$

where
d_{fv}, t_f, w_f, α are illustrated in Figure 6.
$f'c$: concrete specified compressive strength (Mpa)
b_w: section web width
d: section effective depth
A_{sv}: area of transverse reinforcements spaced at s
f_{sy}: yield strength of transverse reinforcements
t_f : center to center spacing of FRP strips
d_{fv}: distance from end of FRP to section extreme tension fiber
n: number of plies of FRP reinforcement
w_f : width of FRP reinforcing plies
t_f: nominal thickness of one ply of FRP reinforcement
E_f: tensile modulus of elasticity of FRP
ε_{fe}: effective strain level in FRP reinforcement attained at failure
ε_{fe} : $0.004 \leq 0.75\varepsilon_{fu}$ (completely wrapped members)
ε_{fe} : $k_v\varepsilon_{fu} \leq 0.004$ (Bonded U-wraps or bonded face plies)
ε_{fu} : ultimate strain capacity of CFRP reinforcement

$$k_v = \frac{k_1 k_2 L_e}{11{,}900\varepsilon_{fu}} \leq 0.75 \text{ ..... (9)}$$

$$L_e = \frac{23{,}300}{(n_f t_f E_f)^{0.58}} \text{ .....(10)}$$

$$k_1 = \left(\frac{f'_c}{27}\right)^{\frac{2}{3}} \text{.....(11)}$$

$$k_2 = \begin{cases} \frac{d_{fv} - L_e}{d_{fv}} & U\text{-}wrap \\ \frac{d_{fv} - L_e}{d_{fv}} & 2\text{-}sides\ bonded \end{cases} \text{ ...(12)}$$

where
L_e : active bond length (mm.)
n_f : modular ratio of elasticity between FRP and concrete = $\frac{E_f}{E_C}$
t_f : nominal thickness of one ply of FRP reinforcement (mm.)

7.2.1.4 Effective strain in FRP laminates

The FRP effective strain is the maximum achievable strain in the FRP system at the nominal strength of the FRP-strengthened reinforced concrete member, as defined by **ACI 440.2R**[53] . The failure mode of both the FRP system and the reinforced concrete member governs this strain. Different configurations of FRP laminates for shear strengthening of reinforced concrete members require different methods for determining the effective strain, as explained in the following subsections.

Fully wrapped members—When FRP

fully wraps reinforced concrete column and beam members, the concrete may lose its aggregate interlock at fiber strains lower than the ultimate fiber strain. To avoid this failure mode, the design strain is restricted to 0.004 for fully wrapped members. This strain limit is based on experimental results **(Priestley et al.1996)** [54] and practical experience. FRP shear-strengthening applications should not use higher strains.

Partially wrapped members or bonded face plies—FRP systems that partially wrap the section (two-sided wraps and U-wraps) or bond to the face of the section may peel off from the concrete before the section loses its aggregate interlock (if they are not properly anchored). Therefore, bond stress analyses have been conducted to assess the effectiveness of these systems and the attainable effective strain level **(Triantafillou, 1998a)** [55] . A bond-reduction factor (k_v) for shear is used to calculate the effective strain. The bond-reduction factor depends on the concrete strength (f'_c), the wrapping scheme (k_2), and the laminate stiffness (L_e -active bond length). **(Khalifa et al. 1998)** [56].

7.2.1.5 Reinforcement limits

The reinforcement should provide a total shear strength equal to the combined shear strength of the FRP and steel reinforcements. The criteria for steel reinforcement only in ACI 318 should be used to limit the shear strength of the reinforcement. Equation 13 expresses this limit.

$$v_s + v_f \leq 0.66\sqrt{f'c}\, b_w d \quad \text{.....(13)}$$

7.2.1.6 Development length

The bond capacity of FRP reinforcement develops over a certain length ldf as research by **Teng et al. (2001)** [57] determined. To mobilize the full effective stress, available anchor length must exceed the calculated value from equation 14, with terms as previously defined.

$$L_{df} = \sqrt{\frac{nE_f t_f}{\sqrt{f'_c}}} \quad \text{..... (14)}$$

7.2.1.7 FRP Strip Spacing

Discrete FRP strips used for shear strengthening need proper coverage for efficiency. The guidelines require center-to-center spacing between strips not exceed d/4 plus the strip width, ensuring sufficient strips cross critical shear planes.

7.2.2 International Federations of Structural Concrete (fib14)

According to fib[58] , to optimize the FRP's effectiveness ,the fiber orientation should be as parallel as possible to the direction of the maximum principal tensile stresses. For beams under shear, this direction forms a (45°)angle with the beam's axis. However , the more common practice is to position the fibers perpendicular to the beam's axis.The total force contributed by the FRP is related to the effective strain induced in the FRP along the principal fiber direction before failure. This effective strain is either a reduced value or a fixed fraction of the FRP's ultimate strain capacity . The effective strain in the FRP never reaches the ultimate strain due to incompatibility between the FRP and cracking in the concrete, which leads to stress concentrations and debonding failure before the FRP can reach its fracture strength. fib14[58]provides equations (15) – (17) to determine the FRP's contribution to the shear capacity of rectangular and T-shaped beam sections.

$$V_{fd} = 0.9\varepsilon_{fd,e} E_{fu} \rho_f b_w d(cot\theta + cot\alpha) sin\alpha$$

..... (15)

$$\rho_f = \begin{cases} \frac{2\, t_f sin\alpha}{b_w} & \text{for continuous reinforcement} \\ \left(\frac{2\, t_f}{b_w}\right)\left(\frac{b_f}{s_f}\right) & \text{for FRP sheets/strips} \end{cases}$$

.....(16)

$$\varepsilon_{fd,e} = K\, \varepsilon_{f,e} \quad \text{.....(17)}$$

K = reduction factor assumed as 0.8.

where:

$\varepsilon_{fd,e}$: design value of effective strain.

E_{fu}: Principal fiber direction elastic modulus of FRP (GPa).
ρ_f :FRP reinforcement ratio.
θ :The assumed angle of the diagonal crack with respect to the mem$_b$er axis is 45 degrees.
α :the angle between the primary orientation of the material fibers and the longitudinal axis of the structural element.
$\varepsilon_{f,e}$:Effective strain in FRP was determined using the formula below :
If the member is fully encased in FRP sheets or adequately anchored, the FRP fracture failure mode governs, and the $\varepsilon_{f,e}$ is calculated using Equation (18). Conversely, if the member is strengthened with FRP U-wraps or side-bonded FRP, the $\varepsilon_{f,e}$ is determined by Equation (19).

$$\varepsilon_{f,e} = 0.17\left(\frac{{f_{cm}}^{2/3}}{E_{fu}\rho_f}\right)^{0.30}\varepsilon_{fu} \quad \text{..... (18)}$$

$$\varepsilon_{f,e} = min\left[0.65\left(\frac{{f_{cm}}^{2/3}}{E_{fu}\rho_f}\right)^{0.56}\times 10^{-3}\,,\ 0.17\left(\frac{{f_{cm}}^{2/3}}{E_{fu}\rho_f}\right)^{0.30}\varepsilon_{fu}\right] \quad \text{..... (19)}$$

where:

f_{cm}: concrete compressive strength (MPa).

To guarantee that all cracks are caught by FRP strips, the maximum spacing (s_f) shouldn't go over $0.9d - b_f/2$ for rectangular sections and $d - h_f - b_f/2$ for T-sections.

7.2.3 Shear Resistance Model by Chen and Teng (2003a, b)

Chen and Teng (2003 a , b)[59] proposed a model to calculate the shear resistance provided by FRP U-wraps, side strips and fully wrapped beams. This model considers the presence of a critical shear crack, which dominates the debonding failure process and is inclined to the beam's longitudinal axis by an angle (θ)(as illustrated in Figure. 7, which shows the general shear strengthening scheme for a beam). The FRP wraps surrounding this shear crack experience varying stress, which is captured by a stress distribution factor. The total shear resistance, (V_{FRP}), contributed by the FRP system is based on the variable shear crack inclination angle (θ) and can be expressed by the following equation:

$$V_{FRP} = 2\, f_{FRP,e}\, t_{FRP} w_{FRP}\, \frac{h_{FRP,e}}{s_{FRP}}\,(cot\theta + cot\beta)sin\beta \quad \text{..... (20).}$$

Where
$f_{FRP,e}$: is the effective stress in the FRP at the ultimate state.
$h_{FRP,e}$:The effective height of the FRP, taken as 0.9 times the beam depth (d).
θ : is the inclination angle of the shear crack, which is assumed as 45 degrees for design.
β :is the angle between the FRP fibres and longitudinal axis of the beam.
For U-wraps, the effective stress in the FRP $f_{FRP,e}$, is determined using the following formula:

$$f_{FRP,e} = D_{FRP}\sigma_{FRP,max} \quad \text{..... (21).}$$

Where (D_{FRP}) is the stress distribution factor and $(\sigma_{FRP,max})$ is the maximum stress at debonding.

D_{FRP} is determined using:

$$D_{FRP} = \begin{cases} \frac{2}{\pi\lambda}\frac{1-cos\frac{\pi}{2}\lambda}{sin\frac{\pi}{2}\lambda} & if\ \lambda \le 1 \\ 1 - \frac{\pi-2}{\pi\lambda} & if\ \lambda > 1 \end{cases} \quad \text{..... (23)}$$

$\sigma_{FRP,max}$ is defined as:

$$\boldsymbol{\sigma_{FRP,max}} = min\begin{cases} f_{FRP} \\ 0.427\beta_w\beta_L\sqrt{\frac{E_{FRP}\sqrt{f'_c}}{t_{FRP}}} \end{cases} \quad \text{....(24).}$$

Where:

β_w: strip width ratio factor:

$$\boldsymbol{\beta_w} = \sqrt{\frac{2-w_{FRP}/s_{FRP}sin\beta}{1+w_{FRP}/s_{FRP}sin\beta}} \quad \text{.....(25).}$$

β_L: bond length factor:

$$\boldsymbol{\beta_L} = \begin{cases} 1 & if\ \lambda \ge 1 \\ sin\frac{\pi\lambda}{2} & if\ \lambda < 1 \end{cases} \quad \text{..... (26).}$$

λ :normalized maximum bond length, calculated as:

$\boldsymbol{\lambda} = \frac{L_{max}}{L_e}$.....(27).

Where $L_{max}$is the maximum bond length of the FRP strips intersected by the critical shear crack ($L_{max} = \frac{h_{FRP,e}}{sin\beta}$) and L_e is the **effective bond length**:

$\boldsymbol{L_e} = \sqrt{\frac{E_{FRP}t_{FRP}}{\sqrt{f'_c}}}$ ..... (28).

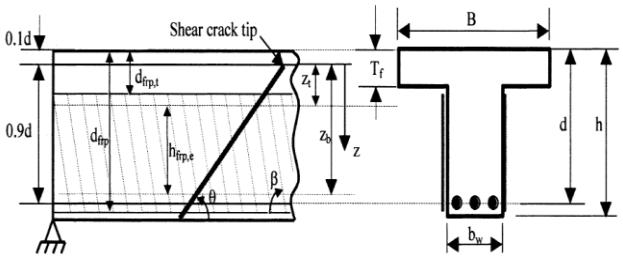

Figure 7. Notation for a general shear strengthening scheme

7.2.4 Intelligent Sensing for Innovative Structures (ISIS) Canada Educational Module 4 – Introduction to FRP-strengthening of concrete structures (ISIS-M04)

The design of shear strengthening for RC beams using FRP is guided by detailed recommendations from organization ISIS Canada Module 4[60]. Typically, FRP is applied externally as U-shaped wraps for beams or full wraps for columns, with U-wraps being more common for beams. This enhances the shear capacity by providing additional transverse reinforcement, similar to the function of steel stirrups. U-wraps help prevent brittle shear failure by bridging cracks. Proper anchorage of U-wraps in the compression zone is essential, often achieved through horizontal FRP strips or alternative anchoring methods to prevent premature debonding. Additionally, rounding beam corners to a minimum radius of 15 mm is necessary to minimize stress concentrations and ensure smooth load transfer between the FRP and the concrete, reducing the risk of localized failure.

The key design equation for the shear resistance (V_r) , is expressed as the sum of the concrete contribution(V_c), steel (V_s) and FRP (V_{frp}),as given in Equation (29):

$V_r = V_c + V_s + V_{frp}$ ..... (29).

$(V_c), (V_s) and\ (V_{frp})$ can be determined using the following equations:

$V_c = 0.2\emptyset_c\sqrt{f'_c}\, b_w d$ ..... (30).

$V_s = \frac{\emptyset_s f_y A_v d}{s}$ ..... (31).

$V_{frp} = \frac{\emptyset_{frp} A_{frp} E_{frp} \varepsilon_{frp} d_{frp}(sin\beta + cos\beta)}{s_{frp}}$ ..... (32).

$A_{frp} = 2t_{frp}w_{frp}$ ..... (33).

The variables and parameters used in the analysis are defined as follows:

- $\emptyset c$: Concrete strength reduction factor, set at 0.6 for buildings and 0.75 for bridges.
- $\emptyset s$: Steel strength reduction factor, with values of 0.85 for buildings and 0.9 for bridges.
- $\emptyset f$: Strength reduction factor for FRP, assigned a value of 0.75 for CFRP and 0.5 for GFRP.
- Ef: Elastic modulus of FRP sheets (measured in MPa).
- β: Inclination angle of FRP sheets (degrees).
- Af: Cross-sectional area of FRP sheets.
- tf: Thickness of FRP sheets (mm).
- wf: Width of FRP sheets (mm).
- sf: Center-to-center spacing of FRP sheets (mm); for continuous wrapping, $sf = wf$.
- df: Distance from the free end of the FRP to the bottom of internal steel stirrups (mm).

Variables wf, sf, df, and β are shown in Figure. 8.

- εf: Effective strain in the FRP, which can be determined using equations (34) - (37).

$\varepsilon_{frpe} = R \cdot \varepsilon_{frpu} \leq 0.004$ ..... (34).

$R = \alpha\lambda_1 \left[\frac{{f'_c}^{2/3}}{\rho_{frp}E_{frp}}\right]^{\lambda_2}$ ..... (35).

$\rho_{frp} = \left(\frac{2t_{frp}}{b_w}\right)\left(\frac{w_{frp}}{s_{frp}}\right)$ ..... (36).

where:
: Set at 0.8.
εf: ultimate strain in FRP.
$\lambda 1$:Equal to 1.35 for CFRP and 1.23 for GFRP.
$\lambda 2$:Equal to 0.30 for CFRP and 0.47 for GFRP.
. Another limit on effective strain in FRP (εf):

$$\varepsilon_{frpe} = \frac{\alpha k_1 k_2 L_e}{9525} \quad \text{..... (37).}$$

$$k_1 = \left[\frac{f'_c}{27.65}\right]^{2/3} \quad \text{..... (38).}$$

$$k_2 = \frac{d_{frp} - n_e L_e}{d_{frp}} \quad \text{..... (39).}$$

$$L_e = \frac{25350}{(t_{frp} E_{frp})^{0.58}} \quad \text{..... (40).}$$

Restricts the maximum center-to-center spacing of FRP strips (s_{frp}) with:

$$s_{frp} \leq w_{frp} + \frac{d}{4}$$

The code restricts the effective strain in the FRP to 0.004 to maintain aggregate interlock and keep crack widths within acceptable limits. Additionally, this strain limit helps to prevent premature bond failure. Furthermore, the code places an upper limit on the total shear resistance in beams, defined as follows:

$V_r \leq V_c + 0.8\lambda \emptyset_c \sqrt{f'_c}\, b_w d$ ..... (41).

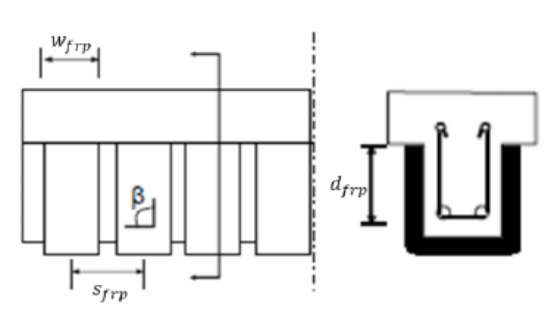

Figure 8. Illustration to define variables: wf, sf, df, and β[60]

8. Existing Research on Basalt Fiber Shear Strengthening

Kar and Biswal (2021) [61] studied the effectiveness of BFRP composites for shear strengthening of RC beams through a comprehensive experimental study and assessed the effect of various variables including strengthening schemes (U-wrapping and full wrapping), orientation of BFRP strips (perpendicular and 45° to the longitudinal axis), type of fibre sheets (basalt and two types of glass fibres), levels of preloading (unloaded, 62 per cent of control beam failure load and load). In order to scrutinise the effectiveness of BFRP for shear strengthening of RC beams, 10 shear-deficient RC beams with dimensions 150 mm wide, 200 mm deep and 2000 mm long, were tested under four-point loading conditions. The experimental results revealed that the failure load of the strengthened beams increased by 17–50 per cent when compared with unstrengthened beams (control of strengthening), and also the toughness (energy to failure) was improved up to 2.74 times. BFRP strips enhanced the shear capacity better by 20 per cent in comparison with glass fibre strips used as sheets. Moreover, based on the experimental results, it is evident that as preload level increases, the enhancement in shear capacity reduces. Several failure modes were observed for different types of wrapping, type and thickness of the fibre sheet, levels of uplifted-load and transverse locations of uplifted-load position. Most of the beams failed in shear after the debonding of FRP strips. In a particularly interesting trial case, the FRP strips failed due to tensile rupture of BFRP strips. Finally , the authors concluded that the basalt fibre sheet can be potentially an alternative to other commonly used fibres for shear strengthening of RCbeams , based on their presented experimental results. Their study also revealed the need for further research to understand the possible degree of variation in the effectiveness of BFRP sheets.

In their (2021) experimental study , **Saribiyik et al**[62]. investigated the shear strengthening of RC beams using BFRP composites. They designed and built 18 RC beam specimens , including three control beams and 15 beams strengthened with BFRP composites in eight different wrapping configurations. These configurations included full wrapping, side bonding, U-shaped strips with and without anchorages, and varying fiber orientation angles of 45° and 90°. The beams were deliberately designed with one shear-deficient region and one region with sufficient shear strength . The researchers used techniques to wrap BFRPs around areas lacking in shear

strength and conducted thorough testing through four point bending , under steady loading until it failed. They measured load, displacement, crack width and shear deformations. The results showed significant improvements in the shear load-carrying capacity of the BFRP strengthened beams compared to the control specimens , with increases ranging from (43% to 100%). The fully wrapped complete strip with a 90° angle (FWCS90) and the fully wrapped strips with a 45° angle (FWS45) exhibited the highest shear strength enhancements, with increases of 100% and 89%, respectively. Additionally , the study observed increased flexural stiffness, reduced crack opening and variable displacement capacities depending on the strengthening method used. The failure mode analysis revealed that in full confinement methods, the BFRP fibers ruptured, whereas in other configurations, debonding occurred due to the tearing of the concrete cover. The researchers discovered , the effectiveness of additional horizontal strips in preventing debonding of the U-shaped strips. They recommended using U-shaped wrapping and side wrapping with anchorages for T-beams , as full wrapping may be difficult to implement.

In an experimental study , **Ahmed M.Sayed (2020**)[63] investigated the shear behavior of large scale RCbeams strengthened with BFRP sheets. The program involved testing six rectangular RC beams, three unstrengthened control specimens and three externally strengthened with four layers of BFRP sheets in a U-jacketing configuration along the shear span. The substantial beams, with heights of (1000 mm) and widths ranging from (300 to 500 mm), were simply supported and subjected to two-point static loading with a shear span-to-depth ratio of (1.90). Rigorous instrumentation, including strain gauges , linear variable displacement transducers (LVDTs), and a data acquisition system, was employed to monitor strains, deflections, and displacements throughout the loading tests. The study aimed to address the limited research on the influence of the critical parameters like beam width, scale effects, and innovative BFRP sheets on the shear strength of RC beams strengthened with externally bonded FRP composites. The findings revealed substantial enhancements in cracking and ultimate load capacities of the BFRP strengthened beams compared to unstrengthened controls , with increases ranging from (1.14 to 1.98) times greater for different beam widths. Furthermore, the depth-to-width ratio influenced the failure angle, lateral strain exhibited an inverse relationship with beam width, and BFRP sheet strain distribution was more uniform in tensile rupture failure modes compared to debonding failures.

Zhang et al. (2023) [64]conducted a study, both experimentally and numerically to investigate the shear behavior of RC beams strengthened with externally bonded BFRP sheets. The experimental program included Three sets of RC beam samples that were tested using four point bending tests; (control group, without BFRP reinforcement) , (with a BFRP bar replacing a steel rebar) and (with BFRP sheets bonded externally on the sides at a 45° angle using epoxy resin). The test results showed that the use of BFRP sheets notably enhanced the shear capacity and ductility of the RC beams. The study concluded that the elastic modulus of the BFRP sheet significantly affects the load capacity and ductility of RC beams, with peak load and midspan displacement increasing linearly with the elastic modulus. Additionally, the sheet bonding area significantly influences the beam's performance, with full-shear section bonding showing the best strengthening effect.

9. Summary

the research studies, dealing with investigating the shear behavior of RC beams, made from normal-strength concrete. The investigations have recently focused on the variables, such as the shear span-to-depth ratio and BFRP use, which has increased the shear capacity and changed failure modes from brittle to more ductile responses.

The most important observation is that the shear span-to-depth plays a very vital role in both the definition of the shear strength and failure characteristics of RC beams: a lower ratio enhances the shear capacity but also

complicates the failure modes, thus necessitating tailored reinforcement strategies that are sensitive to the unique properties of HSC. Another interesting observation regarding the layering of BFRP is that even though there is a significant increase in the beams' ultimate shear strength and ductility with the addition of increasing layers in the wrapping, after a certain number of layers, the benefits do not consistently increase and may even be harmful, like the early debonding kinetics.

Yet, with the significant survey of previous researchers using BFRP in shear strengthening, normal strength concrete cannot always meet the specific requirements that require using HSC, which is very usual in today's construction because of the higher mechanical properties it provides and strict performance demands under shear loading towards any construction. The behavior of HSC under shear loading is undoubtedly going to differ because of the higher compressive strength and a distinct pattern of crack development when it is reinforced with BFRP. This void in the literature requires explicit inquiries into these differences.

There is a growing need for focused research on the interaction of BFRP materials with the denser matrix in HSC. Naturally, this relationship would be essential for optimizing the bonding quality and the long-term efficiency of the reinforcement. Besides that, the number and configuration of BFRP layers need to be optimized toward maximum shear-strengthening advantages in HSC beams without deteriorating their structural integrity. Potential challenges such as stiffness mismatches and the risk of debonding have to be carefully considered.

Future studies should also develop specific strategies for the shear reinforcement that address the unique stress responses and failure characteristics of the HSC. This may involve testing hybrid composites or changing the orientation and properties of the BFRP layers to establish the most efficacious configurations. By filling such research gaps, it is possible to push forward the application of BFRP in high-strength contexts, therefore enhancing safety, durability, and performance in modern concrete structures. As shown in Table 1 and Figure. 9 the experimental results highlight the percentage increases in ultimate shear capacity and the influence of various parameters such as a/d ratios and BFRP layering configurations.

Table 1: Major Parameters of the Collected Experimental Results

References	a\d ratio	Compressive Strength of Concrete (MPa)	Type of FRP	Wrapping Type / angle	Number of Layers	Increase Percentage Relative to Control Beam
Chaallal et al. (1998)[47]	–	20-25	CFRP	Side Strip/ 90°-135°	1 layer	59.09-84.47%
Al-Mussaue et al. (2011)[46]	3.57	12, 20, 30, 39	CFRP	U-wrap/45°	1 layer	18.3-58.3%
Panigrahi et al. (2014)[50]	2.38	22-24	GFRP	Side Strip/ U-wrap with Anchor/90°-45°	2-4 layers	6.17-65.43%
AlShadidi et al. (2016)[51]	3	High Strength (66.5,70.8,73)	GFRP bar and CFRP sheet	Side Strip/ U-wrap /90°-45°	1 layer	129.31-232.76%
Suparp et al. (2019)[48]	1.3	25	Polyester Rope	Full-wrap/90°	1-3 layers	31-52%
Sayed(2020) [63]	1.9	48.75-49.88	BFRP	U-jacketing/90°	4 layers	90.63-97.95%
Kar and Biswal (2021) [61]	3	24.3	BFRP/ GFRP	Full/U-wrap /90°-45°	1 layer	16.9 - 49.6%
Saribiyik et al. (2021)[62]	2.4	16.9	BFRP	Side/ Full / U-wrap /90°-45°	1 layers	43-100%
Zhang et al. (2023)[64]	3.3	35	BFRP bar and sheet	U-wrap /90°	1 layers	10.60%

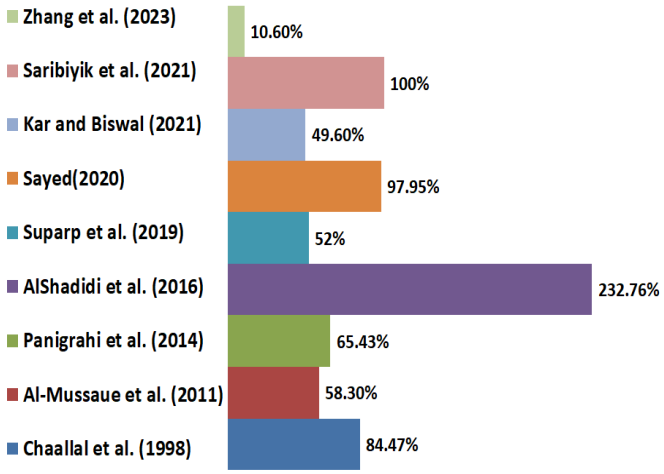

Figure 9. Comparison of Percentage Increase in Shear Capacity Across Studies

References

[1] A. Siddika, M. A. Al Mamun, W. Ferdous, and R. Alyousef, "Performances, challenges and opportunities in strengthening reinforced concrete structures by using FRPs – A state-of-the-art review," *Eng. Fail. Anal.*, vol. 111, p. 104480, 2020, doi:https://doi.org/10.1016/j.engfailanal.2020.104480.

[2] A. Siddika *et al.*, "Flexural performance of wire mesh and geotextile-strengthened reinforced concrete beam," *SN Appl. Sci.*, vol. 1, no. 11, p. 1324, 2019, doi: 10.1007/s42452-019-1373-8.

[3] R. Al-Mahaidi and R. Kalfat, "Chapter 2 - Methods of Structural Rehabilitation and Strengthening," R. Al-Mahaidi and R. B. T.-R. of C. S. with F.-R. P. Kalfat, Eds., Butterworth-Heinemann, 2018, pp. 7–13. doi: https://doi.org/10.1016/B978-0-12-811510-7.00002-1.

[4] D. A. Bournas, A. Pavese, and W. Tizani, "Tensile capacity of FRP anchors in connecting FRP and TRM sheets to concrete," *Eng. Struct.*, vol. 82, pp. 72–81, 2015, doi: https://doi.org/10.1016/j.engstruct.2014.10.031.

[5] C. Cheng and C. Lijuan, "Predicting Flexural Fatigue Performance of RC Beams Strengthened with Externally Bonded FRP due to FRP Debonding," *J. Bridg. Eng.*, vol. 22, no. 11, p. 4017082, Nov. 2017, doi: 10.1061/(ASCE)BE.1943-5592.0001118.

[6] O. A. Hussein and N. N. Khalid, "Behavior of slender RC columns strengthened with partial and full wrapping of BFRP sheet, subjected to variable eccentric loading," *J. Build. Pathol. Rehabil.*, vol. 9, no. 1, p. 48, 2024, doi: 10.1007/s41024-024-00396-5.

[7] E. Monaldo, F. Nerilli, and G. Vairo, "Basalt-based fiber-reinforced materials and structural applications in civil engineering," *Compos. Struct.*, vol. 214, pp. 246–263, 2019.

[8] R. Madotto, N. C. Van Engelen, S. Das, G. Russo, and M. Pauletta, "Shear and flexural strengthening of RC beams using BFRP fabrics," *Eng. Struct.*, vol. 229, p. 111606, 2021.

[9] A. Bastani, S. Das, and D. Lawn, "Rehabilitation of shear deficient steel beams using BFRP fabric," in *Structures*, Elsevier, 2019, pp. 349–361.

[10] V. Fiore, T. Scalici, G. Di Bella, and A. Valenza, "A review on basalt fibre and its composites," *Compos. Part B Eng.*, vol. 74, pp. 74–94, 2015.

[11] J. Sim and C. Park, "Characteristics of basalt fiber as a strengthening material for concrete structures," *Compos. Part B Eng.*, vol. 36, no. 6–7, pp. 504–512, 2005.

[12] S. Jayasuriya, "Experimental Study on Rehabilitation of Corroded Pipes," University of Windsor (Canada), 2017.

[13] H. Jamshaid and R. Mishra, "A green material from rock: basalt fiber--a review," *J. Text. Inst.*, vol. 107, no. 7, pp. 923–937, 2016.

[14] J. Qureshi, "Fibre-Reinforced Polymer (FRP) in Civil Engineering," IntechOpen, 2022.

[15] L. Taerwe, S. Matthys, and others, "FRP reinforcement in RC structures," *Bulletin (Fédération internationale du béton)*, vol. 40. Fédération internationale du Béton (FIB), 2007.

[16] T. Triantafillou *et al.*, "Externally bonded FRP reinforcement for RC structures," *Bulletin FIB*, vol. 14. International Federation for Structural Concrete (fib), 2001.

[17] S. L. Sveinsdóttir, "Experimental research on strengthening of concrete beams by the use of epoxy adhesive and cement-based bonding material," Reykjavík University, 2012. [Online]. Available: http://hdl.handle.net/1946/12546

[18] A. C. I. C. 363, *Guide to quality control and assurance of High-Strength Concrete (ACI 363.2R-11)*. Farmington Hills, MI SE - 19 pages : il. ; 28 cm: ACI Farmington Hills, MI, 2011. doi: LK - https://worldcat.org/title/847870470.

[19] D. Hekmat and S. A. Al-Mashhadi Dalya Hekmat Hameed Asst Student, "Mix Design for High

Strength Concrete With Portland Cement and Silica Fume," *Artic. Int. J. Civ. Eng. Technol.*, vol. 5, no. August, pp. 132–150, 2014, [Online]. Available: www.jifactor.com

[20] M. Yaqub, T. Taxila, I. Bukhari, and T. Taxila, "Development of Mix Design for High Strength Development of Mix Design for High Strength," *Conf. Our World Concr. Struct.*, pp. 31–35, 2006.

[21] A. Annadurai and A. Ravichandran, "Development of mix design for high strength Concrete with Admixtures," *IOSR J. Mech. Civ. Eng.*, vol. 10, no. 5, pp. 22–27, 2014, [Online]. Available: www.iosrjournals.org

[22] A. Cladera and A. R. Marí, "Experimental study on high-strength concrete beams failing in shear," *Eng. Struct.*, vol. 27, no. 10, pp. 1519–1527, 2005, doi: 10.1016/j.engstruct.2005.04.010.

[23] G. Campione, A. Monaco, and G. Minafò, "Shear strength of high-strength concrete beams: Modeling and design recommendations," *Eng. Struct.*, vol. 69, pp. 116–122, 2014, doi: 10.1016/j.engstruct.2014.02.029.

[24] S. Campione, G and Mindess, "No Title Fibers as shear reinforcements for high strength reinforced concrete beams containing stirrups," *Proceeding third Int. HSPFRC – RILEM Work.*, no. Mainz, Germany, pp. 519--529, 1999.

[25] G. Campione, "Role of fibres and stirrups on the experimental behaviour of reinforced concrete beams and flexure and shear," *Proceeding Int. Conf. Compos. Constr.*, 2003.

[26] H. G. Kim, C. Y. Jeong, M. J. Kim, Y. J. Lee, J. H. Park, and K. H. Kim, "Prediction of shear strength of reinforced concrete beams without shear reinforcement considering bond action of longitudinal reinforcements," *Adv. Struct. Eng.*, vol. 21, no. 1, pp. 30–45, 2018, doi: 10.1177/1369433217706778.

[27] M. Słowik, "Shear Failure Mechanism in Concrete Beams," *Procedia Mater. Sci.*, vol. 3, pp. 1977–1982, 2014, doi: 10.1016/j.mspro.2014.06.318.

[28] M. N. Hassoun and A. Al-Manaseer, *Structural concrete: theory and design*. John wiley & sons, 2020.

[29] M. Schmidt, P. Schmidt, S. Wanka, and M. Classen, "Shear response of members without shear reinforcement- experiments and analysis using shear crack propagation theory (SCPT)," *Appl. Sci.*, vol. 11, no. 7, 2021, doi: 10.3390/app11073078.

[30] A. Marì Bernat, N. Spinella, A. Recupero, and A. Cladera, "Mechanical model for the shear strength of steel fiber reinforced concrete (SFRC) beams without stirrups," *Mater. Struct. Constr.*, vol. 53, no. 2, 2020, doi: 10.1617/s11527-020-01461-4.

[31] F. Cavagnis, M. Fernández Ruiz, and A. Muttoni, "Shear failures in reinforced concrete members without transverse reinforcement: An analysis of the critical shear crack development on the basis of test results," *Eng. Struct.*, vol. 103, pp. 157–173, 2015, doi: 10.1016/j.engstruct.2015.09.015.

[32] O. Arowojolu, A. Ibrahim, A. Almakrab, N. Saras, and R. Nielsen, "Influence of Shear Span-to-Effective Depth Ratio on Behavior of High-Strength Reinforced Concrete Beams," *Int. J. Concr. Struct. Mater.*, vol. 15, no. 1, 2021, doi: 10.1186/s40069-020-00444-7.

[33] E. R. Thorhallsson and S. R. Birgisson, "Experiment on concrete beams without shear reinforcement," *4th Int. fib Congr. 2014 Improv. Perform. Concr. Struct. FIB 2014 - Proc.*, pp. 221–224, 2014.

[34] MUTSUYOSHI, S. V. T. J. PERERA, and Hiroshi, "Prediction of Shear Strength of High-Strength Concrete Members Without Web Reinforcement," *Annu. J. Concr. Eng.*, vol. 35, no. 2, pp. 449–504, 2013.

[35] W. K. Alsaraj, L. A. Aljaberi, and H. Y. Alhamdani, "Shear Resistance of Mrpc Lightweight Concrete Beams Without Stirrups," *J. Eng. Sustain. Dev.*, vol. 23, no. 5, pp. 1–11, 2019, doi: 10.31272/jeasd.23.5.1.

[36] D. Plappert, G. C. Ganzenmüller, M. May, and S. Beisel, "Mechanical properties of a unidirectional basalt-fiber/epoxy composite," *J. Compos. Sci.*, vol. 4, no. 3, 2020, doi: 10.3390/jcs4030101.

[37] C. Yuan, W. Chen, T. M. Pham, and H. Hao, "Bond behavior between basalt fibres reinforced polymer sheets and steel fibres reinforced concrete," *Eng. Struct.*, vol. 176, pp. 812–824, 2018, doi: 10.1016/j.engstruct.2018.09.052.

[38] Y. Jianbing, X. Yufeng, L. Saijie, and X. Zhiqiang, "Experimental study on shear performance of basalt fiber concrete beams without web reinforcement," *Case Stud. Constr. Mater.*, vol. 17, no. August, p. e01602, 2022, doi: 10.1016/j.cscm.2022.e01602.

[39] W. He, X. Wang, A. Monier, and Z. Wu, "Shear Behavior of RC Beams Strengthened with Side-Bonded BFRP Grids," *J. Compos. Constr.*, vol. 24, no. 5, pp. 1–13, 2020, doi: 10.1061/(asce)cc.1943-5614.0001069.

[40] B. H. Osman, "Shear Strengthening of Reinforced Concrete (RC) with FRP Sheets Using Different Guidelines," *World J. Eng. Technol.*, vol. 11, no. 02,

pp. 281–292, 2023, doi: 10.4236/wjet.2023.112020.

[41] Rahul S Chaudhari and Swapnil B Gorade, "Investigation on use of basalt fiber reinforced polymer for improvement in flexural strength of reinforcement concrete," *World J. Adv. Eng. Technol. Sci.*, vol. 8, no. 2, pp. 055–061, 2023, doi: 10.30574/wjaets.2023.8.2.0072.

[42] E. Hughes, A. Adesina, B. Paini, S. Das, and N. Van Engelen, "Strengthening of Concrete Beams with Basalt Fibre Reinforced Polymer," in *Structures Congress 2020 - Selected Papers from the Structures Congress 2020*, American Society of Civil Engineers Reston, VA, 2020, pp. 449–456. doi: 10.1061/9780784482896.041.

[43] W. Chen, T. M. Pham, H. Sichembe, L. Chen, and H. Hao, "Experimental study of flexural behaviour of RC beams strengthened by longitudinal and U-shaped basalt FRP sheet," *Compos. Part B Eng.*, vol. 134, pp. 114–126, 2018, doi: 10.1016/j.compositesb.2017.09.053.

[44] H. Surwase, G. N. Narule, and S. B. Walke, "Behavior of RC T-Beam Strengthen Using Basalt Fiber Reinforced Polymer (FRP) Sheet," *Int. Res. J. Eng. Technol.*, vol. 6, no. 6, pp. 3525–3529, 2019, [Online]. Available: www.irjet.net

[45] A. M. H. Kadhim, H. A. Numan, and M. Özakça, "Flexural Strengthening and Rehabilitation of Reinforced Concrete Beam Using BFRP Composites: Finite Element Approach," *Adv. Civ. Eng.*, vol. 2019, 2019, doi: 10.1155/2019/4981750.

[46] A. I. S. Al-mussaue, "Behavior of Concrete Beams Reinforced in Shear," *J. Eng.*, vol. 17, no. 1, pp. 46–61, 2011.

[47] O. Chaallal, M.-J. Nollet, and D. Perraton, "Shear Strengthening of RC Beams by Externally Bonded Side CFRP Strips," *J. Compos. Constr.*, vol. 2, no. 2, pp. 111–113, 1998, doi: 10.1061/(asce)1090-0268(1998)2:2(111).

[48] S. Suparp, P. Joyklad, and Q. Hussain, "Shear Strengthening of RC Beams Using Polyester Rope," *Int. J. Eng. Technol.*, vol. 11, no. 4, pp. 267–272, 2019, doi: 10.7763/ijet.2019.v11.1159.

[49] H. H. Mhanna, R. A. Hawileh, and J. A. Abdalla, "Shear strengthening of reinforced concrete beams using CFRP wraps," *Procedia Struct. Integr.*, vol. 17, pp. 214–221, 2019, doi: 10.1016/j.prostr.2019.08.029.

[50] A. K. Panigrahi, K. C. Biswal, and M. R. Barik, "Strengthening of shear deficient RC T-beams with externally bonded GFRP sheets," *Constr. Build. Mater.*, vol. 57, pp. 81–91, 2014, doi: 10.1016/j.conbuildmat.2014.01.076.

[51] E. Lec and E. Lec, "Shear Behavior of High Strength Concrete Beams Reinforced with GFRP Bars and Strengthened by CFRP," *J. Eng. Dev.*, vol. 20, no. 1, pp. 1–18, 2016.

[52] ACI Committee 440, *ACI 440. 2R-17 Guide for the Design and Construction of Externally Bonded FRP Systems for Strengthening Concrete Structures*. in ACI (Collection). American Concrete Institute, Farmington Hills (MI), 2017.

[53] K. Soudki and T. Alkhrdaji, *Guide for the Design and Construction of Externally Bonded FRP Systems for Strengthening Concrete Structures (ACI 440.2R-02)*. 2005. doi: 10.1061/40753(171)159.

[54] K. Kawashima, *Seismic design and retrofit of bridges*, vol. 33, no. 3. John Wiley & Sons, 2000. doi: 10.5459/bnzsee.33.3.265-285.

[55] T. C. Triantafillou, "Shear strengthening of reinforced concrete beams using epoxy-bonded FRP composites," *ACI Struct. J.*, vol. 95, no. 2, pp. 107–115, 1998, doi: 10.14359/531.

[56] A. Khalifa, W. J. Gold, A. Nanni, and A. A. M.I., "Contribution of Externally Bonded FRP to Shear Capacity of RC Flexural Members," *J. Compos. Constr.*, vol. 2, no. 4, pp. 195–202, 1998, doi: 10.1061/(asce)1090-0268(1998)2:4(195).

[57] J. G. Teng, S. T. Smith, J. Yao, and J. F. Chen, "Intermediate crack-induced debonding in RC beams and slabs," *Constr. Build. Mater.*, vol. 17, no. 6–7, pp. 447–462, 2003, doi: 10.1016/S0950-0618(03)00043-6.

[58] fib Bulletin No. 14, "Externally bonded FRP reinforcement for RC structures," *Tech. Report, Fed. Int. Du Béton, Fr.*, vol. 14, p. 138, 2001.

[59] J. F. Chen and J. G. Teng, "Shear capacity of FRP-strengthened RC beams: FRP debonding," *Constr. Build. Mater.*, vol. 17, no. 1, pp. 27–41, 2003, doi: https://doi.org/10.1016/S0950-0618(02)00091-0.

[60] ISIS Education Committee, "ISIS Educational Module 4: An Introduction to FRP Strengthening of Concrete Structures," *Intell. Sens. Innov. Winnipeg*, pp. 1–54, 2010.

[61] S. Kar and K. C. Biswal, "External shear strengthening of RC beams with basalt fiber sheets: An experimental study," in *Structures*, Elsevier, 2021, pp. 305–315. doi: 10.1016/j.istruc.2021.01.094.

[62] A. Saribiyik, B. Abodan, and M. T. Balci, "Experimental study on shear strengthening of RC beams with basalt FRP strips using different

wrapping methods," *Eng. Sci. Technol. an Int. J.*, vol. 24, no. 1, pp. 192–204, 2021, doi: 10.1016/j.jestch.2020.06.003.

[63] A. M. Sayed, "Experimental study of large-scale RC beams shear-strengthened with basalt FRP sheets," *Civ. Eng. J.*, vol. 6, no. 4, pp. 769–784, 2020, doi: 10.28991/cej-2020-03091507.

[64] W. Zhang, S. Kang, Y. Huang, and X. Liu, "Behavior of Reinforced Concrete Beams without Stirrups and Strengthened with Basalt Fiber–Reinforced Polymer Sheets," *J. Compos. Constr.*, vol. 27, no. 2, pp. 1–16, 2023, doi: 10.1061/jccof2.cceng-4082.